SELECTION AND COORDINATION OF SURGE ARRESTERS FOR SWITCHING TRANSIENT MITIGATION IN PHOTOVOLTAIC POWER PLANTS

R. Oliveira*, P. Bokoro*, B. Paul* and E. Ndlovu**

* *Department of Electrical and Electronic Technology, University of Johannesburg (Doornfontein Campus), P.O Box 524, Auckland Park, South Africa, Email: 201315138@student.uj.ac.za; pitshoub@uj.ac.za; bspaul@uj.ac.za*

** *Pele Energy Group, 3 Centex close, Eastgate Kramerville, Sandton, 2196, South Africa, Email: elen@peleenergygroup.com*

Abstract: Photovoltaic energy generation has become a popular renewable alternative to conventional energy generation that utilise fossil fuels. However, given the diversity and complexity of these PV plants, it is imperative that such plant equipment be protected against the greatest contributor to equipment failure; surges. Software simulation using EMTP-RV version 3.3, this paper implements a proposed methodology for the insulation coordination study of a PV plant. The overvoltages associated with the opening of vacuum circuit breakers, at various test points along the network are considered in order to recommend possible selection criteria of surge arresters as well as location thereof. The study finds that for a reduction of surge magnitudes from 8 p.u to within 1.2 p.u would require surge arrester energy capabilities to be greater than 2.8 kJ/kV for the medium voltage (MV) arresters , and capabilities exceeding 259kJ/kV for the low voltage (LV) arrester. For the high voltage (HV) section of the plant, no surge propagation was identified thus exempting it from the insulation coordination. The above mentioned, along with surge current and overvoltage levels comprise the findings of the study providing parameter guidelines for arrester selection.

Keywords: Insulation Coordination, PV, Surge arresters, EMTP-RV

1. INTRODUCTION

With major focus on renewable energy, PV solar has become a more sought after and implemented form of renewable energy generation in South Africa. With the introduction of the Renewable Energy Independent Power Producer Procurement Program (REIPPPP), large international and national companies have invested great capital in these plants [1]. In order to maximise the return on investment, maintenance on the plant must be at the lowest cost possible, with the longevity of the plant being a key priority. This implies taking all necessary precautions to protect the system from damage.

Damage to network equipment may be, and is often contributed to surges as a result of Vacuum Circuit Breaker (VCB) switching as they generate very fast-fronted overvoltages (VFFOs) [2, 3]. These surges become of great concern when considering the nature of a PV power plant. A PV plant is more complex than conventional, prime-mover employed power plants in terms of electrical diversity; the PV plant takes sun generated potential in the form of a DC voltage, converting it to AC and transforming it with its many inverters and transformers. Protection of network equipment against overvoltages employs the use of Surge Protection Devices (SPDs) such as metal oxide (MO) surge arresters. The aim of these devices are to clamp the surges to within the Basic Impulse Level (BIL) of the equipment to be protected.

2. PV PLANT LAYOUT AND PARAMETERS

The PV plant layout considered in this study is based on a generic representation of a portion of the complete PV plant, as a direct result of restrictions imposed by EMTP educational licence, limiting the number of components implementable. The considered layout is depicted in figure 1 below.

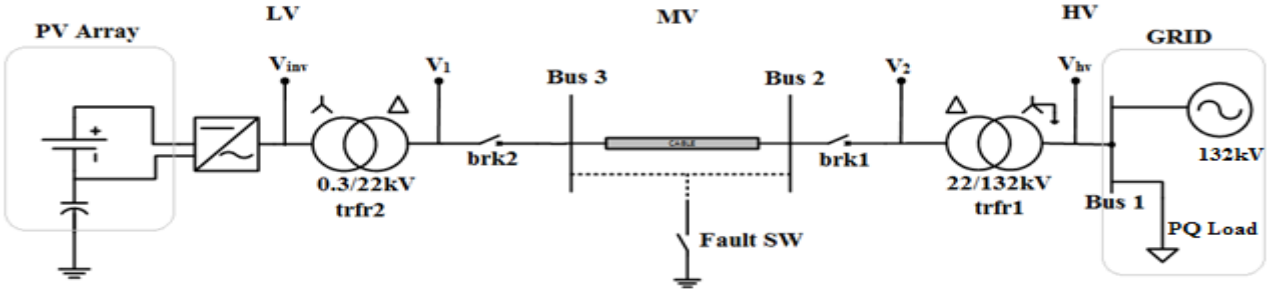

Figure 1: The PV Plant layout considered

The network particulars taken are summarised in table 1

Table 1: Network Parameters taken for simulation

Description	Constituents	Parameters
PV Array	Ideal DC Voltage source.	1000VDC; C = 1nF
Inverter	PWM Based DC to AC Converter	• VDC_{MAX} = 1000V • VAC = $300V_{RMS}$ • P_{out} = 1.4MW
Transformer trfr2	2-winding Transformer	• Configuration: YD • 0.3/22kV • $X^{"}$ = 6%
Cable	MV XLPE Insulated Power Cable	• Length: 240m • R= 0.1 Ω/km • C= 0.367 μF • X_L= 0.094 Ω/km • $300mm^2$
Transformer trfr1	2-winding transformer	• Configuration: DYg • 22/132kV • $X^{"}$ = 11%
Grid	3-phase AC source (Slack) Lumped load	• 132kV • P = 650 kW • Q = 800 kVar

It must be noted at this point that the stray capacitance of the PV power plant had been neglected. Furthermore, the breakers, brk1 and brk2 were the only breakers considered at the medium voltage (MV) level, and were assumed to only operate as part of the protection scheme implemented in the network. As such the breakers operate under fault conditions, and thus when opened, disconnect under fault levels. The faults implemented were typical earth faults as they are considered more commonly to occur and pose great fault current levels. Their respective switching is discussed in greater detail under the methodology of the study. Lastly, it was noted that various lengths of cable were encountered from the inverter container fields (between bus 3 and bus 2). It is well documented that cables, due to their reactive properties are capable of mitigating the transients imposed on an electrical network [3, 4]. Hence the shortest cable found in the network was selected in order to observe the maximum transient levels at the Medium-Voltage (MV) level.

3. METHODOLOGY

The approach to the analysis of the switching transients employed in this study closely follows the recommended procedure provided in [5]. The outcomes of the study were furthermore correlate with the arrester classification as stipulated in [6]. The methodology is summarised in the flowchart provided in figure 2 below. The conduction of this study made use of EMTP-RV v3.3 for simulation and analysis purposes, as it is renowned for its transient observation capabilities.

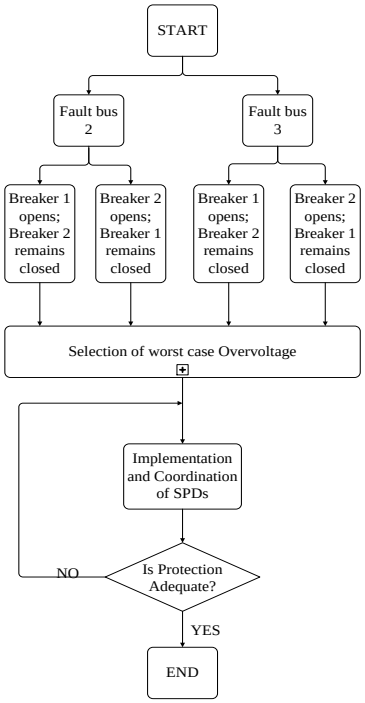

Figure 2: Flowchart summarising the methodology employed

With reference to the figure above, every branch of the flowchart was explored. Considering case 1 for instance; firstly, an earth fault was placed on bus 2. A typical earth fault was chosen due to its characteristically large fault current magnitude. The fault was initiated through an ideal switch between the fault points (chosen to be bus 2 and 3) and earth. An arbitrary time of 0.3 seconds was chosen for the occurrence of the fault. The breaker, brk1, was then opened in a mean time of 40ms after the occurrence of the fault, while maintaining breaker brk2 closed. However, given that the breaker may open at any point within a period of the supply voltage, random breaker operating times were employed within the desired tripping time. This was possible through a statistical study of overvoltage at each of the test points over 15 randomly timed simulations, with respect to each case considered. This value of 15 simulations was selected in order to obtain supporting and sufficient information for analysis. Apart from the difference in actual breaker operating time, each simulation executed involved a time-domain simulation for which a time-step of 1μs, over a period of 1 second, was chosen for the study. Similarly for the second possible case, with bus 2 under fault. Breaker brk1 was maintained closed, while breaker brk2 was set to open 40 ms after the occurrence of the fault. The above two cases were then repeated, however, with respect to a fault at bus 3. This produced four cases of analysis from which the worst case could be isolated for further analysis. Upon determination of the worst case overvoltages, the simulation number representing the maximum overvoltage could then be isolated and simulated under a time-domain analysis. In this analysis, surge arresters were then employed as a means of overvoltage mitigation, defined by their energy absorption requirements, overvoltage levels and current levels.

4. RESULTS AND DISCUSSION

4.1. Statistical analysis results

The statistical study was required to determine under which circumstances the maximum overvoltage would be developed, as well as the probability of such surges occurring at each instance of breaker operation under typical earth fault conditions. Table 2 below provides details of the cases executed, indicating a reference to the resulting figures to follow.

Table 2: Switching scenarios implemented in simulation

Simulation Case	Fault Location	Breaker operation
Case 1	Bus 2	Brk1 open (0.34s) Brk2 closed
Case 2	Bus 2	Brk2 open (0.34s) Brk1 closed
Case 3	Bus 3	Brk1 open (0.34s) Brk2 closed
Case 4	Bus 3	Brk2 open (0.34s) Brk1 closed

The statistical study on the above cases revealed that the maximum overvoltage was presented under simulation case 4. The resulting maximum overvoltages levels experienced in this case are presented in bar chart form in figure 3 below.

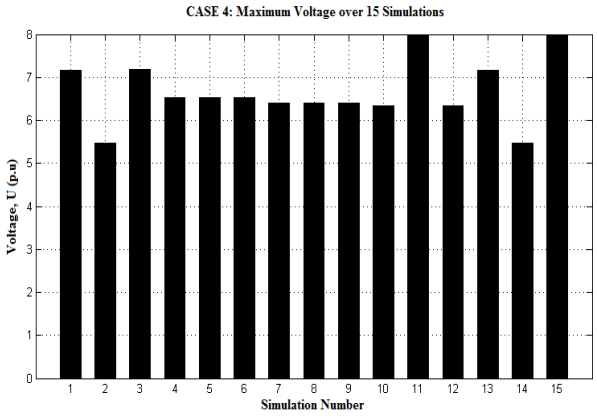

Figure 3: Bar chart depicting the maximum overvoltages over 15 simulations (case 4)

For this case a maximum of 8.p.u was encountered twice over the 15 simulations, with no simulation yielding less than 5 p.u. The maximum overvoltages were encountered in simulation number 11 and 15, of which 11 was chosen to represent the worst case overvoltage data. Conduction of an identical analysis for the remaining cases 1 to 3 revealed the range of maximum overvoltages as provided in table 3.

Table 3: Resulting Overvoltages from statistical Study

Simulation Case	Max/Min range over 15 simulations	Overvoltage (p.u)
Case 1	Max.	3.55
	Min.	1.9
Case 2	Max.	7
	Min.	4.7
Case 3	Max.	2.2
	Min.	1.7
Case 4	Max.	8
	Min.	5.5

From the table above, it was deduced that the operation of breaker brk2 produced the larger overvoltages when compared to the remaining two cases involving brk1. In addition, as it was determined that case 4 resulted in the greatest overvoltage, it was used as the worst case scenario for further analysis and comparison purposes. As such a cumulative distribution function was executed with respect to this case, yielding the graph shown in figure 4 below.

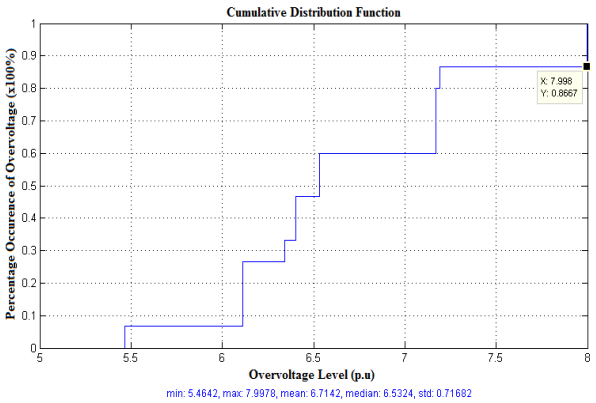

Figure 4: Cumulative distribution function of overvoltage with respect to case 4.

Figure 4 above highlights the probability of occurrence of the overvoltage and its magnitude based on the statistical data provided in figure 3. It was found that there was an 86.67% probability of encountering an overvoltage of less than 7.9978 p.u, with no probability of encountering a surge of less than 5.4642 p.u.

4.2. Time-domain analysis of worst case (Case 4)

Under the time-domain analysis, simulation number 11 of case 4 was selected as the reference for fixed random data simulation in EMTP-RV. In doing so, it allowed the contributions to this high overvoltage to be analysed more closely. To achieve this, the voltage with respect to time at each test point was plotted an analysed to determine the point of greatest overvoltage. The 8 p.u surge was detected at test point V_1, its plot is shown below in figure 5.

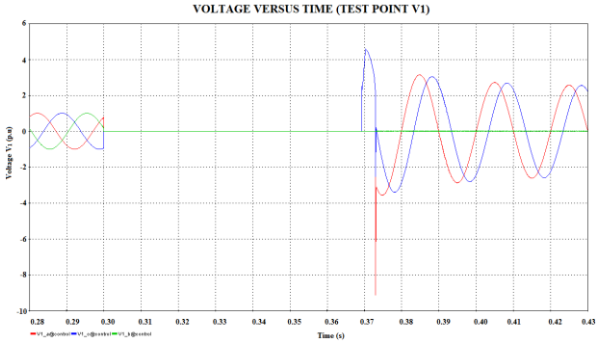

Figure 5: Voltage versus Time (No SPD) at Test point

It can been seen that the main contributor to the maximum overvoltage encountered was as a direct result of the fault being located nearest to test point V_1 and breaker brk2, yielding a surge magnitude of 8 p.u for phase A, and above 4 p.u for phase B. A likewise analysis into the remaining test points revealed their respective contributions in terms of overvoltage. This is provided in table 4 below

Table 4: Overvoltage with respect to test point

Test Point	Overvoltage (p.u)
$\mathbf{V_{INV}}$	3
$\mathbf{V_1}$	8
$\mathbf{V_2}$	1.95
$\mathbf{V_{hv}}$	1

With respect to the table above, it was found that the surge, as a result of brk2 operation, propagated into the LV section of the plant according to test point V_{INV}. Furthermore, it was noted that at test point V_2, an overvoltage of 1.95 p.u was seen however as a result of the occurrence of the fault rather than that of brk2 operation. It was also found that there was no propagation of the surge into the HV section of the plant, despite minor distortion to phase C as a result of the earth fault.

4.3. Implementation and Coordination of Surge Arrester

Taking into consideration the findings above, the approach was to firstly mitigate the maximum surge presented. This was achieved by placing a surge arrester at test point V_1, between transformer trfr2 and bus 3. Although effective in mitigating the surge experienced at test point V_1, it was found to be insufficient in preventing the surges found at test points V_{INV} and V_2. Consequently, the implementation of surge arresters at these test points was required, coordinated with the surge arrester implemented at test point V_1. This notion is shown in figure 6 below.

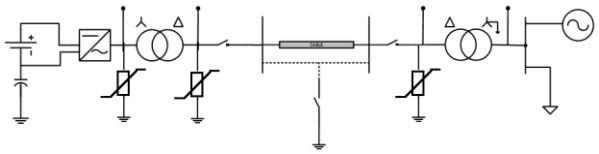

Figure 6: Network with MO surge arresters implemented

Surge arrester models were placed at the test points V_{INV}, V_1 and V_2 as shown in figure 6 above. This approach was found to be successful in mitigating the overvoltages encountered, not only at test point V_1 but at the remaining test points as well, clamping the surges to 1.2 p.u and below. An example of this mitigation at V_1 is shown in the voltage versus time plot in figure 7 below.

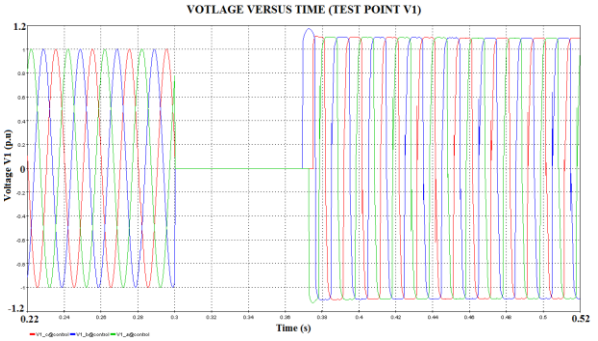

Figure 7: Voltage versus time at Test point V_1.

In order to verify the protection level offered by the implementation of the surge arresters, a statistical analysis was again performed, considering 15 simulations as before. The results of the statistical analysis are provided in figure 8 below.

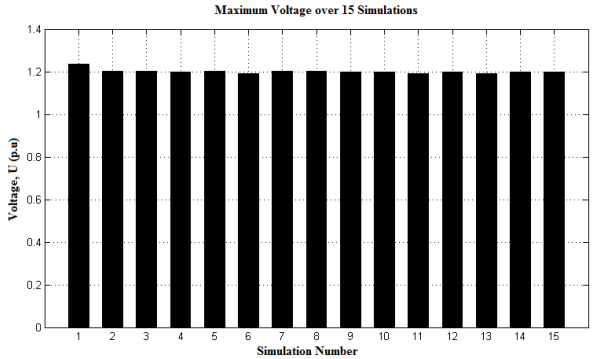

Figure 8: Maximum network p.u overvoltage over 15 simulations

The bar chart in figure 8 above demonstrates the effectiveness of surge arresters in maintaining the presented surges within 1.2 p.u at the four test points throughout the network. Consequently, the resulting cumulative distribution of these results are provided in figure 9 below.

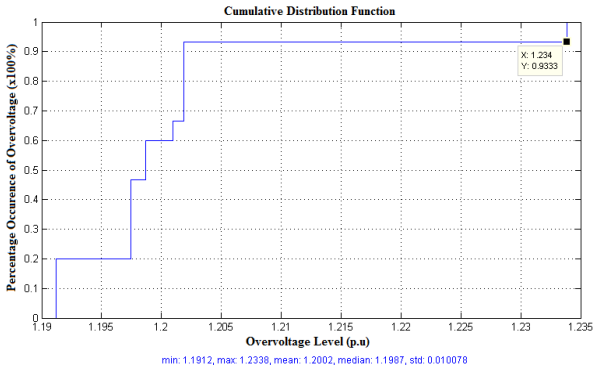

Figure 9: Cumulative distribution function of overvoltage with respect to implemented surge protection

From the cumulative distribution function above it was found that a there was a 93.33% probability of experiencing surges with a magnitude less than 1.234 p.u. The above results indicated the importance and necessity of implementing surge arresters as a means of ensuring system longevity and stability. The arrester criteria to achieve this protection level was then to be determined as presented in the section to follow.

4.4. Arrester Selection Criteria

Knowing the maximum p.u voltage encountered in the PV network, along with the proposed location of the surge arresters, the class of surge arrester could then be suggested based on the energy absorbed by the arresters as well as their surge current under simulation. The energy with respect to the surge arresters at their respective locations were analysed in the time-domain as was done for the overvoltage. Considering the arrester placed at test point V_1, its energy versus time plot is shown in figure 10 below.

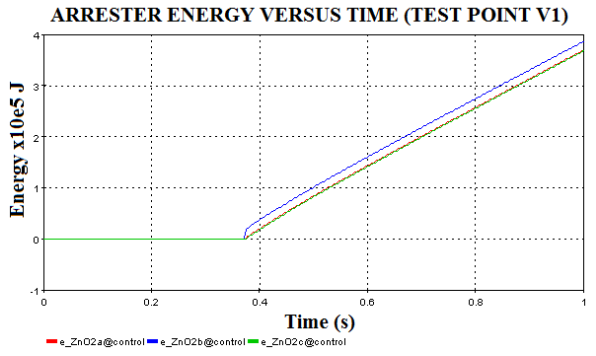

Figure 10: Arrester Energy with respect to Time at test point V_1.

It was determined from the graph above that the energy absorption capabilities of the arrester would have to withstand energy levels of up to 400kJ at test points V1. A similar analysis into the energy capability of the arresters at test points V_{INV} and V_2 revealed peak energy requirements of 160kJ and 41kJ respectively. At this stage of the analysis, the thermal energy rating (or Energy capability) of the arresters was calculated using the following relationship outlined in equation 1 below

$$W_{th} = \frac{E(kJ)}{[(V_{pu} * kV_{base}) - U_r]} \quad (1)$$

Where

- W_{th} is the thermal energy rating
- $V_{p.u}$ is the p.u Overvoltage measured at the test point of interest
- kV_{base} is the nominal/base voltage with respect to the location (300V for LV and 22kV for MV or U_s may be taken)
- U_s is the nominal operating voltage of the relevant section of the network
- U_r is the rated operating voltage of the surge arrester

The p.u overvoltages as presented in table 4, along with U_r of the arresters (taken as 1.2 x U_s) were implemented in equation 1. The resulting minimum energy capability of the arresters were found to be 259.259 kJ/kV for arrestor at location V_{INV}, 2.685kJ/kV for arrestor at V_1 and 2.579kJ/kV for arrester at V_2. The latter two were found to be achievable according to the arrestor classification in [6], however concerns had been raised regarding the energy capability required for the LV arrester at V_{INV}.

Along with the energy capability of the arresters, their surge current was analysed. The current versus time plot of the arrester located at V_1 is shown in figure 11 below.

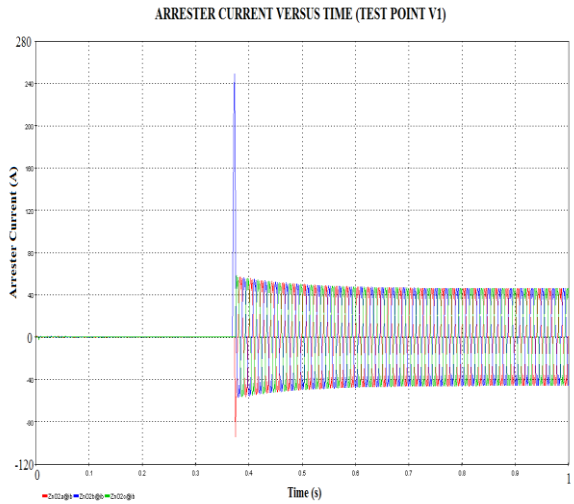

Figure 11: Surge current versus time at test point V_1

A look into the surge current presented in the plot above indicated a peak surge current of 250A. The surge currents encountered at V_{INV} and V_2 were found to be 10kA and 510A respectively. The resulting surge arrester selection criteria, deduced from the obtained results presented in this document, are provided in table 5 below.

Table 5: Surge Arrester Selection criteria

Test Point	Overvoltage			Arrester Rated Voltage U_r (kV_{RMS})	Nominal Operation Voltage U_m (kV_{RMS})	Peak Arrester Energy Absorption (kJ)	Energy Capability W_{th} (kJ/kV-U_r)	Surge Current (kA)
	No SPD (p.u)	No SPD (kV_{RMS})	Surge Arrester at V_{INV}, V_1 and V_2 (p.u)					
V_{INV}	3,00	0.900	1,23	0.36	0.30	140	259	10
V_1	8,00	176	1,20	27	22	400	2,69	0, 25
V_2	1,95	43	1,20	27	22	41	2,58	0, 51
V_w	1,00	132	1,00	-	132	-	-	-

The information was evaluated with the intended purpose of providing guidance in the selection process of suitable arresters to mitigate the transient surges presented in the PV plant simulated. The tabulated results above, suggest class 2 surge arresters as possible candidates to achieving the necessary insulation protection of the plant.

5. CONCLUSIONS

Through the simulation and analysis of four possible MV breaker switching scenarios, the maximum overvoltage presented was found to be due to breaker brk2 opening as a direct result of an earth-fault at bus 3. The overvoltage generated was found to be in the region of 8 p.u, much larger than an expected overvoltage of approximately 3 p.u. Further analysis into the contributions found that the surge also propagated into the LV section of the plant. No evidence was found regarding the propagation of the surge into the HV section. Consequently, the surge arrester criteria developed through the results was found to restrict the entire network overvoltage to 1.2 p.u, with a probability of 93.33% chance of a surge having a magnitude of 1.234 p.u or less, from a probability of 86.67% encountering a surge of 7.998 p.u. Assuming a basic switching impulse insulation level (BSL) of 1.2 p.u for the plant equipment would imply successful protection. The thermal energy ratings required of the arresters, in order to achieve the above mentioned protection, were found to be 259 kJ/kV, 2.69 kJ/kV 2.58kJ/kV for arresters at test points V_{INV}, V_1 and V_2 respectively. The results obtained through this study merely provide a guideline of parameter values to ensure successful mitigation of switching impulses in PV plants. Concluding, indeed circuit breakers imposed transients into the network as a result of opening operations, and furthermore that arresters with the minimum requirements as stipulated by the finding would be able to mitigate these transient surges, possibly class 2 surge arresters. However, much work can still be performed, and is encouraged, specifically regarding the LV section of the plant. Its complex equipment requires further modelling enhancements to improve the accuracy of the obtained results.

REFERENCES

[1] Eberhard, A., Kolker, J. and Leigland, J. *South Africa's renewable energy IPP procurement program: Success factors and lessons*. (2014)

[2] McDermit, Daniel C. et al. "Medium-Voltage Switching Transient-Induced Potential Transformer Failures: Prediction, Measurement, And Practical Solutions". *IEEE Transactions on Industry Applications* 49.4, p1726-1737. (2013).

[3] Cox, P., Hayes, H.L., Hopkinson, P.J., Piteo, R. and Boggs, S.A. *Surge protective properties of medium voltage underground cable*. (2006) Available at: http://faculty.ims.uconn.edu/~eprcable/ref22.pdf (Accessed: 28 August 2016.

[4] Kuczek, T. and Florkowski, M. *Zeszyty Naukowe Wydziału Elektrotechniki i Automatyki Politechniki Gdańskiej Nr 36 Vacuum Circuit Breaker Switching in Photovoltaic Power Plants – Overvoltage Analysis for Various Topologies and Network Conditions*. (2015)

[5] SANS 60099-5: Surge Arresters – *Part 5: Selection and application recommendations,* (2013)

[6] SANS 60099-4: Surge Arresters – *Part 4: Metal-oxide surge arresters without gaps for a.c. systems,* 2013.